

Numerical Simulation of The Impact of Chorda Tendinea Rapture on the Mitral Valve Leaflets Stress by Finite Element Method

HASAN ABEDINI¹ and ADEL JOHARI MOGHADAM^{2*}

¹Department of Biomedical Engineering , Amir Kabir University, Tehran, Iran.

²Department of Cardiology , AJA University of Medical Sciences, Tehran, Iran.

*Corresponding author E-mail : adeljoharim@yahoo.com

<http://dx.doi.org/10.13005/bpj/930>

(Received: February 10, 2016; accepted: March 13, 2016)

ABSTRACT

Numerical modeling of the lack of blood supply in mitral valve regurgitation and its related surgeries are very attractive, because it enables us to examine whether the surgery would improve the blood flow to reduce the tension in tissues. This is crucial, because the negative effects of increasing tension can only be determined over time. However, a finite element method is valuable. This requires accurate heart geometries, heart tissue parameters, a powerful solver and etc. In the present study, with the help of simulation, the function of mitral valve was compared in both modes of normal and valve prolapsed, through which useful results were obtained. Among the models, hyper-elastic Mooney-Rivlin model is used for the first time. The boundary conditions of model are also much nearby to the reality of ventricular function in imposing pressure on the valves. Unlike previous models, in which the prolapse was never been significant, the function of valve is carefully studied and compared in this model. The findings, at the end of the simulation, suggest that the prolapse caused by the rupture of chorda tendinea can be problematic to the valve function. Although the number of chorda tendinea and their properties can be very different in each individual, what has been suggested as a possibility in the results of this simulation is that in the rupture of chorda tendinea, since the imposed tension on the other chorda tendinea and also the tensions created on the leaflets increase, the modification of chorda tendinea as quickly as possible prevents the rupture of other cords. Therefore, the replacement of artificial valve which is very costly and risky may be avoided with a timely surgery.

Keywords: Mitral valve leaflets, Chorda tendinea, finite element method, mitral valve prolapse

INTRODUCTION

Heart diseases is one of the most common death cause worldwide¹. Simplifying of the heart geometry and tissues microstructure which are interacted with solids and fluids increase our knowledge of fluids dynamic in heart which is necessary for mechanical analysis of heart and surgeries. In fact, by imaging of the heart which can be done by removing the heart from the body, just high quality images would be obtained. Due to difference of the heart geometry inside and outside of the body, this would be a challenging issue. The next major obstacle in the prediction of the analysis

is the lack of mechanical impact of heart valves. The sever impact of heart valves on fluid dynamic is obvious².

The most important mechanical coupling which is between ventricle and heart valves caused by chorda tendinea which connect the free edges of front and rear leaflets to the muscles and thus to the left ventricle wall²⁻³.

Leaking backward of blood is a clinical pathology involved the mitral valve and left ventricle with dynamic interaction between solids and fluids. Blood backflow to the left atrium in systole phase

due to the changes in blood flow in heart and valves. This backflow causes lung swell and slight changes in the final volume left ventricular that is associated with mortality⁴. Modification of blood backflow to reduce myocardium tension and slow/stop ventricular changes are the main goal of surgeries for this disorder. Numerical models of blood backflow and their modification are used to predict successful outcomes of surgeries to reduce tensions and improvement of blood flow².

In general, a proper three-dimensional model will be needed for three-dimensional modeling and analysis of the mitral valve. The geometry of mitral valve was checked and entered to Catia software, after extracting of basic information from articles. The model was imported into the 3D finite element software (ADINA) and boundary condition was determined after specifying the valve properties and components, and finally the model was analyzed⁵. Extraction of stresses and strains were the outcome of this model analysis⁶.

METHODS

Equations

The solid object equation is shown below. (Equation 1)

$$\tau + f^B = \rho_s \ddot{u}$$

Equation 1

Solid object equation. δ : Tension, f^B : Physical force, ρ_s : Density of solid object, \ddot{u} : Acceleration

$$M(t + \Delta t)\ddot{U} + C(t + \Delta t)\dot{U} + K(t)U = R(t + \Delta t) - F(t)$$

Kinematics system should also be considered in order to achieve proper finite element form to apply solid model equation. A solid object with high mobility and low strain was assumed for the kinematics of this study model. Nonlinear dynamic equation (Equation 2) would be the most appropriate system to applying equations due to high mobility of assumed solid object^{7, 8}.

Equation 2

Nonlinear dynamic equation. M : Mass matrix, C : Damping matrix, K : Stiffness matrix, R : External force vector, F : External force vector equal

to the tension elements in the previous iteration, \ddot{U} : Acceleration of solid object nodes, \dot{U} : Speed of solid object nodes, U : Displacement of solid object nodes

The F term in above equation was used to calculate nonlinear terms of the system. The F vector contains physical force, focused force, surface force, and primary stresses. M , C , and K matrices considered constant and shown in Equation 3.

$$M = \sum_i \int_{v(i)} \rho_i H_i^T H_i dV_i$$

$$C = \sum_i \int_{v(i)} k_i H_i^T H_i dV_i$$

$$K = \sum_i \int_{v(i)} B_i^T C_i B_i dV_i$$

Equation 3- M , C , and K matrices. i : Element number. η : Elements' density, k : Elements' dumping activity coefficient, H : Element displacement element, B : Strain-displacement matrix of element, C : Elasticity matrix of element, V : Volume of element.

There should be a special attention to degree of freedom when a solid object has been modeled. All rotational freedom degrees should be considered equal to zero to achieve convergence, if in a particular model only movement freedom degree taken into consideration. Suitable element should also selected for solid object to discretization of finite element method equations. When the boundary condition, material properties, element, and network applied correctly, solid model equations would be fully resolved. Newtonian method is used to linearize the system of equations and finally as fluid equations, solving sparse would be used for these linear system⁹.

Numerical simulation

Valve geometry include annulus ring, leaflets, and tendons. Annulus would be investigated first. Annulus ring is roughly oval in

shape¹⁰. Different models of valves are provided in various articles based on photos which are shown some of them in figure 1A. Although annulus ring is a dynamic part of heart valve, but a fixed geometry was assumed for it to reduce the complexity of this study's issue. An oval shape hole was considered for annulus profile. Figure 1B is a proposed annulus profile by Kevin Daniel Lau which is used in this study¹¹.

The article of Emilliano Votta was also used to leaflets design. Leaflets can be considered as a surface with approximately 1mm thickness due to their in consequential thickness¹². Although there is disagreement about thickness of leaflets in various studies, but 1mm thickness is offered in all of them. The thickness of front and rear leaflets considered equal in this study which is corresponds to the reality with a little error. The form and angle of surfaces toward horizon of leaflets are shown in figure 2. The front leaflet is bigger than rear one but allocate smaller part of the annulus. This leaflet is monolithic. The rear leaflet consists three section and the middle one is bigger than others.

The leaflet can be easily designed based on figure 2. Tendinous cords were also drawn as shown in this figure.

Thus, the geometry of valve was designed on Catia software based on figure 2 and the sizes which are calculated in articles and prepared for finite element analysis. The resulting design is shown in figure 3.

Mitral valve properties

Biomechanical behavioral measures of soft tissues require a careful definition of basic models which are need assessment of histologic and morphologic characteristics of desired tissue. Mechanical experimental tests face many operational problems. Therefore, numerical methods are easier way. Expert models which are associated with experimental data should be accepted considering to the nonlinear behavior of the materials¹³.

Heart valve tissue is soft and hydrated. Stress-strain responses are their macroscopic result of their microscopic structure. The tissue of

valves' leaflets are formed by elastic matrix which are reinforced by collagen fibers. Tissues and their behaviors intended hyperelastic to analyze their large deformation. Hyperelastic materials have nonlinear stress-strain curve and large strains. Most of biologic tissues are hyperelastic.

If the presence of strain energy density function could be assumed for an object, this material would be hyperelastic. Hyperelastic materials defined by energy function and also invariants of C matrix which is obtained from F transformation matrix. Strain energy function would be $W=W(C)$, if proper amount of strain assumed. In this function, C is the right Cauchy Green tensor and C function is $C=FTF$ which F in this equation is transformation gradient. According to these, stress-strain curve function is shown below.

$$S = 2\partial W/\partial C$$

Equation 4- Stress-strain curve function. S: The second Piola- Kirchhoff stress tensor

If the material being homogeneous, it can be shown that the strain energy function will be depend on C by their main invariables:

$$W = W(I_1, I_2, I_3)$$

$$I_1 = trC, I_2 = 1/2[tr(C^2) - I_1^2], I_3 = detC$$

Order structure of soft tissues, such as the presence of fibroids with specific space direction, determines the heterogeneous mechanical response of tissue. This fact can be calculated by checking the previous formula, the introduction of new invariants, which these invariants are directly related to the structure of tissue.

For example, consider the presence of a fibers family in a particular direction in a small area of a tissue! Two more invariables will be introduced:

$$I_4 = A \cdot CA, I_5 = A \cdot C^2A$$

A is a unit vector that indicates the direction of fibers in no deformation state. The local direction of deformed state will be indicated by unit vector, $a=FA/\dot{\epsilon}$, which $\dot{\epsilon}$ represents the strain in fibers direction. The fourth invariable is square strain of tissue in fibers direction, while the fifth one will be

calculated for the ratio of fibers to strain energy function which is depended on shear and direction of fibers. Thus, strain energy function and stress-strain equation will be equation 5.

$$W = W(I_1, I_2, I_3, I_4, I_5)$$

$$S = 2 \sum_{i=1}^5 [(\partial W / \partial I_i)(\partial I_i / \partial C)]$$

Equation 5- Strain energy function and stress-strain equation

Basic model defined by the above equations are symmetrical and homogeneous, and usually use for many ideas and soft tissue mechanics. There is various models such as Ogden, Mooney-Rivlin, Polynomial, Reduced polynomial, Arruda-Boyce, Marlow Neo, and etc. for hyperelastic materials. A specific energy function is defined for all of these models and their coefficients will be determined.

Mooney-Rivlin hyperelastic 9 nominal model was used in this simulation for the first time. The model's *W* strain energy function is shown below.

$$W = C_1(I_1 - 3) + C_2(I_2 - 3) + C_3(I_1 - 3)^2 + C_4(I_1 - 3)(I_2 - 3) + C_5(I_2 - 3)^2 + C_6(I_1 - 3)^3 + C_7(I_1 - 3)^2(I_2 - 3) + C_8(I_1 - 3)(I_2 - 3)^2 + C_9(I_2 - 3)^3$$

In this function, *I*₁ and *I*₂ are invariables of *C*_{ij} Cauchy Green deformation matrices:

$$I_1 = C_{kk}, I_2 = \frac{1}{2} [I_1^2 - C_{ij}C_{ij}]$$

C1 to C9 are also constants of matter. These constants obtained from curve fitting to the experimental data of heart valves tissues stress-strain data which are reported by Yin and May-Newman¹⁴ and given below.

At first, the charts obtained from loading heart valves tissues is shown in figure 4. This graph is taken from Yin and May-Newman results of heart valves tissue tests¹⁵.

The graph and desired model coefficients are shown in figure 5 and table 1.

Due to high elasticity of tendons, they assumed elastic and linear. According to the paper by Votta, 16 Mpa and 0.45 were intended for Yang modulus and Poisson ratio of tendons. The model is elastic and isotropic. With these properties, desired model can be entered into the finite element software. ADINA ver. 8.8 was used for this study.

Uploading and boundary condition

Annulus ring was intended fix for boundary condition. Outer surfaces have systolic pressure and the inner ones have atrial pressure. Its diagram is shown in figure 6.

The used elements were triangular. Settings were intended for large deformation and convergence of the subject. The number of steps were 8022 and the minimum E-4 time step was 1.24667581. The total time for solving was 8245.47s (Hⁿ 2.5 hours). The number of triangular elements were 46210. The valve shape before analysis is shown in figure 7.

RESULTS AND DISCUSSION

First, the valve function was analyzed in normal mode. The results showed normal function of valve in this mode, according to the physiologic boundary condition. Stresses and strains of valve were derived on various times conditions in the analysis. Analyzing the normal function of valve can be used as a standard for comparison of its operation in healthy and damaged mode of valve¹⁶.

Table 1: Mooney-Rivlin Coefficients

Variable	Coefficients
C1	25517.1736493095
C2	19445.8910349734
C3	13126.1671986812
C4	10352.3090759319
C5	8151.7905945757
C6	5488.58097719279
C7	4376.38022869666
C8	3487.18987844141
C9	2776.6605548665

The bulk modulus : 44963064.6842829

Mitral valve performance analysis

As it shown in figure 8, primary tension is significantly high near the annulus and it increases by the time. With closure of the mitral valve, sever tension will be observed in parts of leaflets which are near the annulus. There is also sever strains in these parts.

The reason of this phenomenon is clear. A sever tension inserted to the high deformable tissue of valve and therefore the leaflets next to the annulus will be severely deformed. Valves' strain in various times are shown in figure 9.

After rising the tension in these regions, the tension is severely reduced in free edges of valve which was expected.

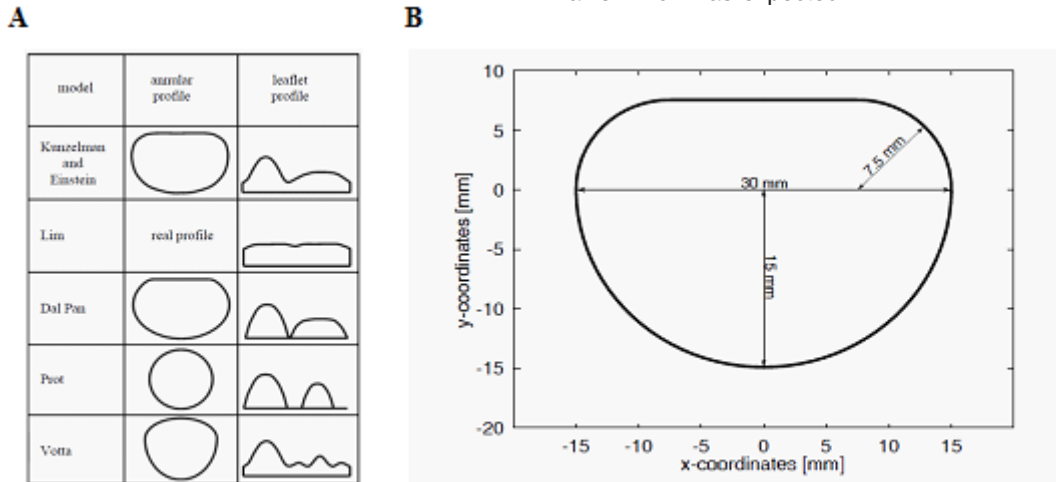


Fig. 1: (A) Various profiles for annulus. B) The annulus profile used in this study

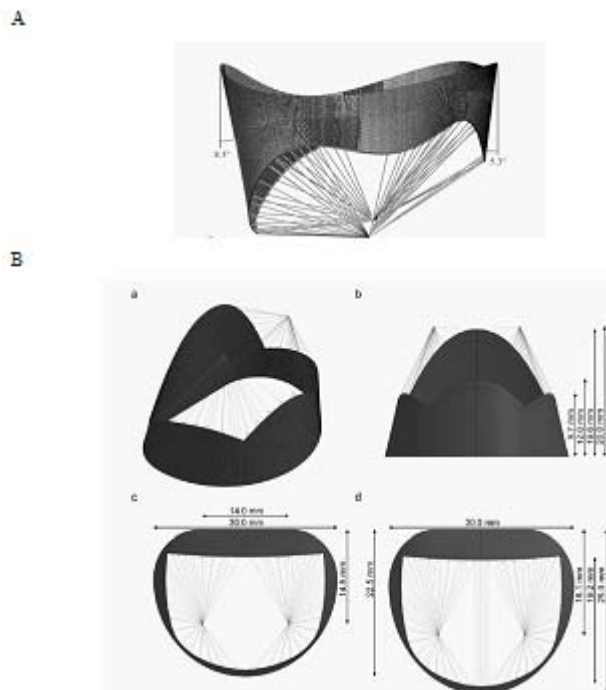


Fig. 2: (A) Side view of valve. B) Dimensions of valve

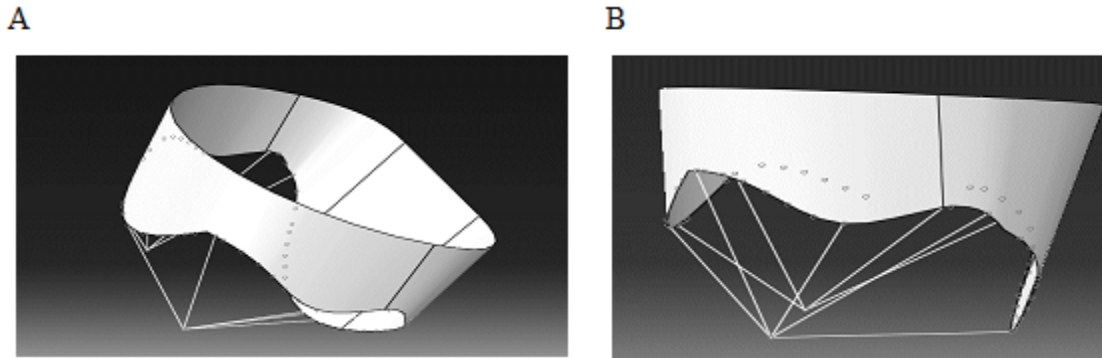


Fig. 3: The geometry of leaflet based on Catia

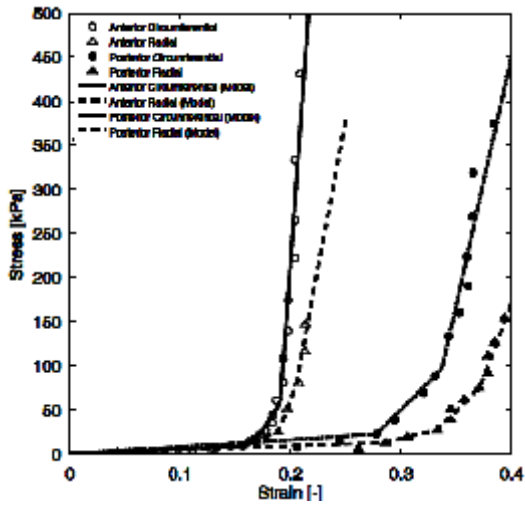


Fig. 4: Stress-strain curve of valve tissue

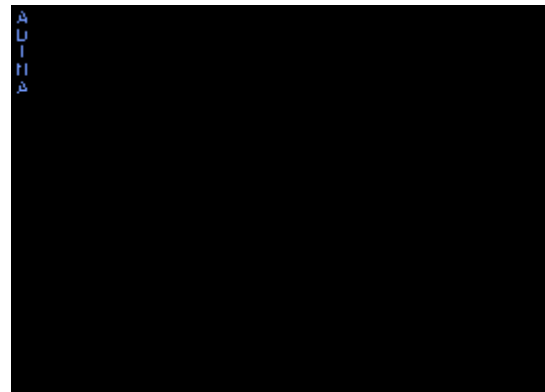


Fig. 5: Stress-strain curve of used model

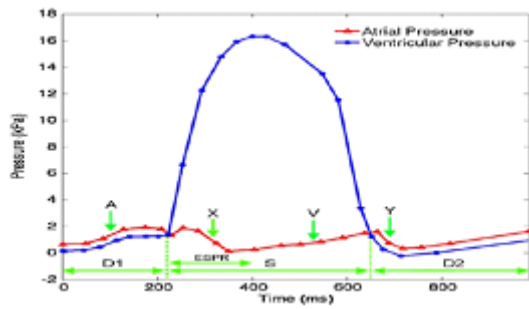


Fig. 6: Atrial and Ventricular pressure

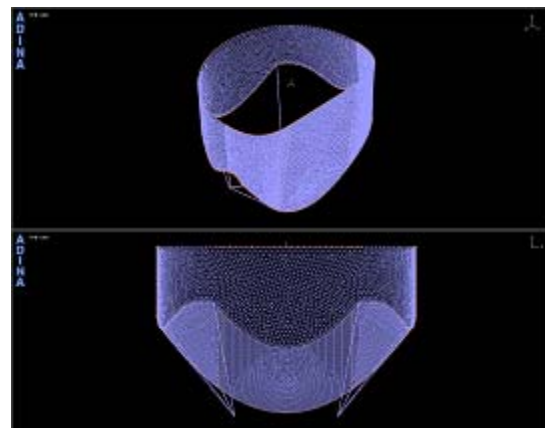


Fig. 7: The finite element model of valve

Another important point in this analysis is the tension in chorda tendinea and connection point of them to the leaflets. The beneficial and important role of these chorda tendinea in proper form of valve to have acceptable and accurate closure can be observed in figure 8 and 9. It is notable that the tension in chorda tendinea is so much lower than valve. Chorda tendinea will have lower deformity

rather than valve due to higher elasticity of their tissue than valve tissue.

Valve performance analysis in rupture mode (Prolapse)

In next step, as it said before, the valve performance was analyzed in rupture mode. For this, some tendons assumed damaged. The results

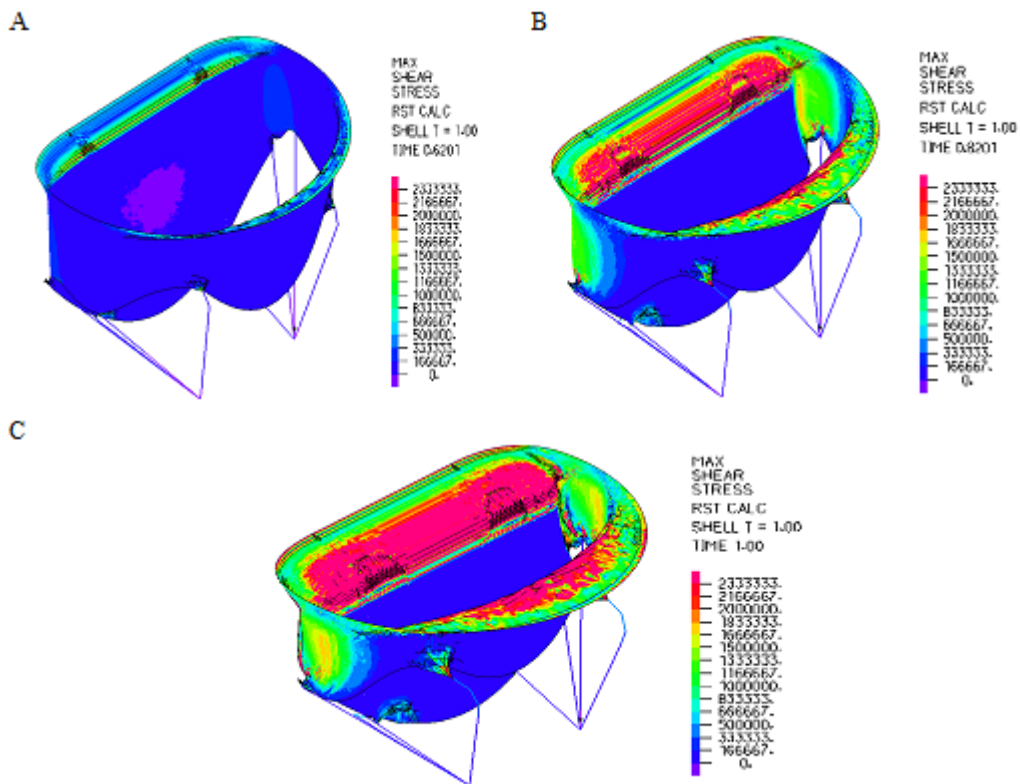


Fig. 8: The maximum of shear stress for normal valve in various times. A) $t=0.6s$, B) $t=0.8s$, and C) $t=1s$

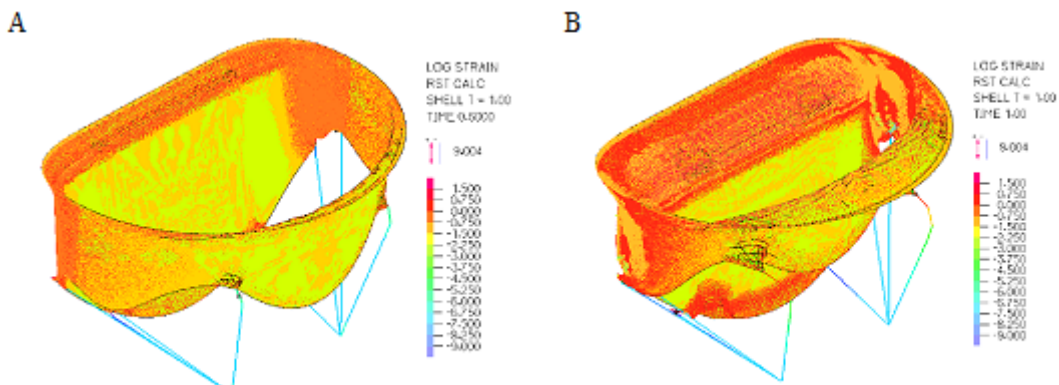


Fig. 9: Logarithmic strain of normal valve in various times. A) $t=0.6s$ and B) $t=1s$

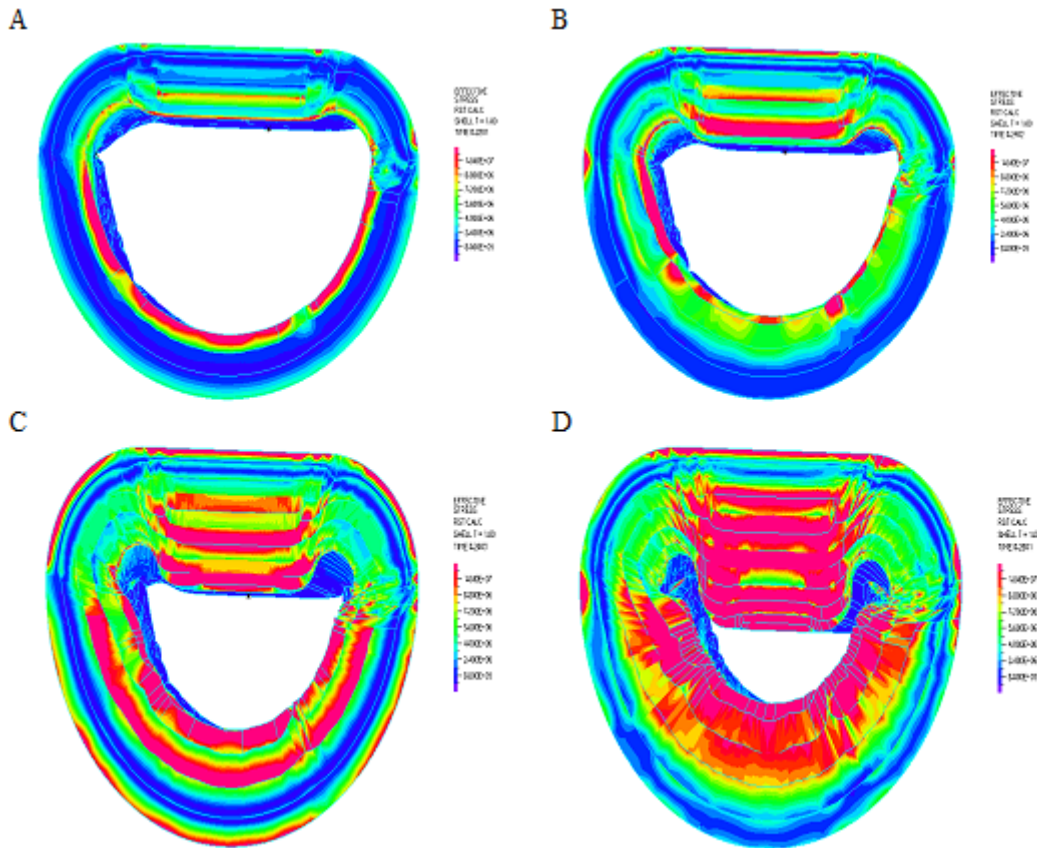


Fig. 10: Effective tension on prolapse mode in various times. A) t=0.2s, B) t=0.6s, C) t=0.8s, and D) t=1s

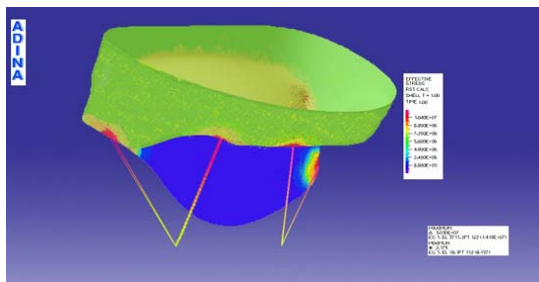


Fig. 11: The effective tension on chorda tendinea in prolapse mode after 1sec

showed different tension in leaflets and chorda tendinea. Figure 10 shows the effect of tension on damaged valve and the chorda tendinea response is shown in figure 11. The simulation was done by ADINA software.

As it shown in above analysis, in prolapse mode due to chorda tendinea (it was shown by reduction in chorda tendinea number in this

simulation), or in the absence of required number of chorda tendinea, leaflets will choose optional form and face to abnormal distortion and finally the tension will increase in them sharply. The clear and sharp tension has been seen in comparison of this mode and normal mode in contour tension. According to the obtained results and analysis, there would be an open pore in the middle of leaflets which indicates the failure of leaflets in completely closure and prevention of blood flow from ventricle to atrium in prolapse mode.

The analysis showed, if the size of mitral valve which caused more than 38 mm² (approximately), the suffered individual will be survive up to 5 years. Previously it was anticipated that a person can have more longevity. So by an engineering perspective, if a mitral valve pore area in prolapse reach about 38 mm², surgery has been recommended. In prolapse, the tension in leaflets and chorda tendinea will be more than crisis and

would cause unpredictable risks. Each people have specific number of chorda tendinea and this factor has been omitted in this study due to investigation the leaflets tension and measuring the pores size. Our results showed when the mitral valve pore area reach 38mm², the tension in chorda tendinea would be critical and after that the chorda tendinea will be rapture due to heart cycle. On the other hand, due to analyzing the tensions of mitral valve leaflets in prolapse and contour of the tension in leaflets, the critical points could be specify for surgery.

CONCLUSION

This method can show the position of leaflets with high tension, so this method would be a powerful measuring tool for physicians, during or prior of surgery, to show critical location of leaflets for focusing during the surgery. It will be expected that most experienced physicians would be have more successful surgery by using this method.

REFERENCES

1. A.S. Go, D. Mozaffarian, V.L. Roger, E.J. Benjamin, J.D. Berry, W.B. Borden, D.M. Bravata, S. Dai, E.S. Ford, C.S. Fox, Heart disease and stroke statistics—2013 update: a report from the American Heart Association. *Circulation* **127**: e6 (2013).
2. D.R. Einstein, F. Del Pin, X. Jiao, A.P. Kuprat, J.P. Carson, K.S. Kunzelman, R.P. Cochran, J.M. Guccione, M.B. Ratcliffe, Fluid–structure interactions of the mitral valve and left heart: comprehensive strategies, past, present and future. *International Journal for Numerical Methods in Biomedical Engineering* **26**: 348-380 (2010).
3. H. Muresian, The clinical anatomy of the mitral valve. *Clinical anatomy* **22**: 85-98 (2009).
4. L.A. Piérard, P. Lancellotti, The role of ischemic mitral regurgitation in the pathogenesis of acute pulmonary edema. *New England Journal of Medicine* **351**: 1627-1634 (2004).
5. K. Kunzelman, R. Cochran, C. Chuong, W. Ring, E. Verrier, R. Eberhart, Finite element analysis of the mitral valve. *The Journal of heart valve disease* **2**: 326-340 (1993).
6. H. Zhang, X. Zhang, S. Ji, Y. Guo, G. Ledezma, N. Elabbasi, Recent development of fluid–structure interaction capabilities in the ADINA system. *Computers & structures* **81**: 1071-1085 (2003).
7. M. Stevanella, E. Votta, A. Redaelli, Mitral valve finite element modeling: implications of tissues' nonlinear response and annular motion. *Journal of biomechanical engineering* **131**: 121010 (2009).
8. T. Mansi, I. Voigt, B. Georgescu, X. Zheng, E.A. Mengue, M. Hackl, R.I. Ionasec, T. Noack, J. Seeburger, D. Comaniciu, An integrated framework for finite-element modeling of mitral valve biomechanics from medical images: application to MitralClip intervention planning. *Medical image analysis* **16**: 1330-1346 (2012).
9. K. Bathe, Theory and Modeling Guide, Vol III: ADINA-F, ADINA R&D. Inc, Watertown, MA (2003).
10. V. Prot, R. Haaverstad, B. Skallerud, Finite element analysis of the mitral apparatus: annulus shape effect and chordal force distribution. *Biomechanics and modeling in mechanobiology* **8**: 43-55 (2009).
11. K. Lau, V. Diaz, P. Scambler, G. Burriesci, Mitral valve dynamics in structural and fluid–structure interaction models. *Medical engineering & physics* **32**: 1057-1064 (2010).
12. E. Votta, E. Caiani, F. Veronesi, M. Soncini, F.M. Montevecchi, A. Redaelli, Mitral valve finite-element modelling from ultrasound data: a pilot study for a new approach to understand mitral function and clinical scenarios. *Philosophical Transactions of the Royal Society of London A: Mathematical, Physical and Engineering Sciences* **366**: 3411-3434 (2008).
13. V. Prot, B. Skallerud, Nonlinear solid finite element analysis of mitral valves with heterogeneous leaflet layers. *Computational Mechanics* **43**: 353-368 (2009).

14. K. May-Newman, F. Yin, Biaxial mechanical behavior of excised porcine mitral valve leaflets. *American Journal of Physiology-Heart and Circulatory Physiology* **269**: H1319-H1327 (1995).
15. K. May-Newman, F. Yin, A constitutive law for mitral valve tissue. *Journal of biomechanical engineering* **120**: 38-47 (1998).
16. E. Yellin, S. Laniado, C. Peskin, R. Frater, Analysis and interpretation of the normal mitral valve flow curve. *The mitral valve* 163-172 (1976).